ELSEVIER

Journal of Alloys and Compounds 317–318 (2001) 19–25

Journal of ALLOYS AND COMPOUNDS

www.elsevier.com/locate/jallcom

Phase equilibria and diffusion paths in the Ti–Al–O–N system

H.J. Seifert*, A. Kussmaul, F. Aldinger

Max-Planck-Institut für Metallforschung and Institut für Nichtmetallische Anorganische Materialien, Universität Stuttgart, Pulvermetallurgisches Laboratorium, Heisenbergstr. 5, D-70569 Stuttgart, Germany

Abstract

To provide a basis for the calculation of high-temperature phase reactions in the Ti–Al–O–N system a thermodynamic dataset using the CALPHAD method (CALculation of PHAse Diagrams) was developed. Analytical Gibbs energy descriptions for the system phases were taken from literature or optimized in this work. The solid solution series Al_2TiO_5–Ti_3O_5 (tialite) was modeled with the sublattice description $(Al^{+3},Ti^{+3},Ti^{+4})_2(Al^{+3},Ti^{+3},Ti^{+4})_1(O^{-2})_5$. The nine energy parameters resulting from the applied Compound Energy Formalism could be reduced to four independent parameters. Reciprocal reactions and the condition of electroneutrality were taken into account. Based on the optimized binary and ternary phase diagrams extrapolating calculations on quaternary compositions were carried out and compared with experimental work. The results show good agreement with the phase assemblages in the microstructure of ceramics in the Ti–Al–O–N system. Additionally, the oxidation behavior of γ-TiAl can be explained qualitatively.

Keywords: Ti–Al–O–N system; Phase equilibria; CALPHAD; Multiphase ceramics; Oxidation

1. Introduction

Compounds of titanium in the Ti–Al–O–N system are most important for the development of a large variety of commercially important refractory materials. Titaniumnitride, titaniumoxides, titaniumoxinitrides and tialites of the solid solution series (Al_2TiO_5–Ti_3O_5) together with other phases of the system establish the microstructure of multiphase ceramics with outstanding high-temperature properties [1]. Adjusting the materials physico-chemical and mechanical properties to specific technical demands requires processing temperatures higher than 1500°C and well-selected sintering atmospheres. The efficient development of such materials necessitates detailed information on phase equilibria and phase reactions in the Ti–Al–O–N system under reducing and oxidizing conditions. Such phase equilibria information is essential also for the understanding of the oxidation behavior of γ-TiAl based alloys in air. Due to their good mechanical properties in combination with low densities such alloys are technically important materials for high temperature applications. However, the oxidation resistance of these metallic materials has still to be improved and is presently under intensive investigation [2].

Fig. 1 shows the concentration tetrahedron for the Ti–Al–O–N system. The solid phases stable at 1000 K are indicated. Other stoichiometric and solution phases appearing at higher temperatures are listed in Table 1. The numerous appearing phases illustrate the difficulty to explore phase reactions and stabilities only by experiments. Thus computational phase studies are helpful. However, this requires comprehensive modeling of involved solution phases and reliable thermodynamic

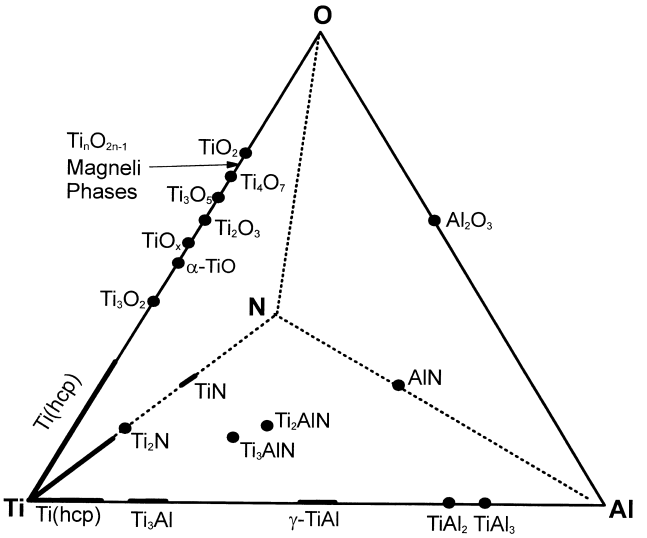

Fig. 1. Solid phases in the Ti–Al–O–N system ($T = 1000$ K).

*Corresponding author.

0925-8388/01/$ – see front matter
PII: S0925-8388(00)01409-2

Table 1
Solid phases in the Ti–Al–O–N system only stable at temperatures higher than 1000 K

Binary phases	Ternary phases
δ-Ti_xAl_y	Al_2TiO_5–Ti_3O_5 (ss)
Ti_4N_3	$Al_6Ti_2O_{15}$
Ti_3N_2	$Ti_3Al_2N_2$
	TiO_x–TiN_x
	AlON (spinel)
	AlON (21R, 27R, 12H, ...)

datasets. The crystal structure of the solution phases and the chemical behavior of the constituting elements under varying physico-chemical conditions have to be taken into account. Particularly the treatment of oxide systems including transition elements requires the consideration of changing ion valencies with varying oxygen potential. The way of modeling and thermodynamic calculation of such systems is shown by example of the Ti–Al–O–N system.

2. Thermodynamic calculations

Thermodynamic calculations using the CALPHAD-method (CALculation of PHAse Diagrams) have proved to be a powerful tool to investigate multicomponent systems and predict phase equilibria even in experimentally unexplored systems [3,4]. That approach was used in this work and different phase diagrams and property diagrams were calculated using the software of Lukas [5] and Thermo-Calc [6].

The thermodynamic descriptions for the binary and ternary subsystems were partly taken from literature and partly derived within the scope of our work on the quaternary Ti–Al–O–N system. The descriptions for the binary systems Ti–Al, Ti–N, Al–O and O–N (gaseous species) were taken from literature [7–10]. The data for the Ti–O system were partially adopted from a recent assessment by Lee [11]. However, the model description and parameters for the liquid phase and TiO were modified to achieve compatibility with other subsystems. Additionally, the description for the phases TiO_2 and Ti_4O_7 had to be refined according to phase diagram information not taken into account by [11]. The Al–N system was taken from an earlier optimization in our group [12]. The optimization of the ternary subsystem Ti–Al–O [13] was partially accepted and extended by modeling the ternary solid solution phase Al_2TiO_5–Ti_3O_5 (tialite) as described below. Due to the lack of experimental data, one single thermodynamic description was developed for the different modifications of Al_2TiO_5 and Ti_3O_5, respectively. Additionally, an experimentally established ternary phase ('X') was introduced. The ternary Ti–O–N system was optimized. The descriptions for the Ti–Al–N and the Al–O–N systems were accepted from literature [14,15]. All binary and ternary thermodynamic descriptions were combined in a single database to calculate and predict the phase equilibria and reactions in the quaternary system Ti–Al–O–N by extrapolation. The full dataset is available from [16] and also stored in the SGTE database [10].

3. Ternary system Ti–Al–O

The calculated partial phase diagram of the Ti–O system is shown in Fig. 2. Depending on the redox conditions titanium shows different valency states in the oxides, e.g. $Ti(III)_2O_3$, $(Ti(III,IV))_3O_5$, $(Ti(III,IV))_4O_7$ and $Ti(IV)O_2$. Due to a lack of thermodynamic data the Magneli-phases were not described. The calculated isothermal section of the Ti–Al–O system at a temperature of 1173 K is shown in Fig. 3. The phases hcp-Ti and α_2-Ti_3Al show extended solubilities for oxygen. Less oxygen can be dissolved in γ-TiAl. α-Al_2O_3 is in equilibrium with all other phases at this temperature, besides bcc-Ti. Following experimental information the ternary X-phase is treated as a stoichiometric phase. The tialite solid solution extends from composition Ti_3O_5 to $Ti_{1.9}Al_{1.1}O_5$. This solid solution range of tialite expands with increasing temperature. At T=1573 K it reaches the limiting composition Al_2TiO_5, aluminum titanate, located in the pseudobinary subsystem TiO_2–Al_2O_3. At p_{O_2}=1 bar the thermodynamically optimized phase boundaries of this subsystem are shown in Fig. 4. They are in fair agreement with experimental data. The liquidus line deviates to some extent. However, in this system the liquidus is difficult to measure and some of the experimental data obviously are influenced by systematic errors. These data were not taken into account for the optimization. Details on the optimization procedure are given in [16].

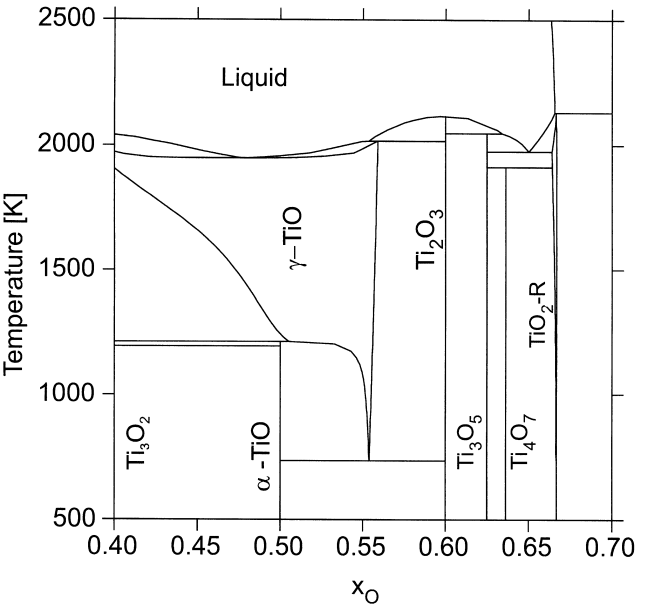

Fig. 2. Partial phase diagram of the Ti–O system.

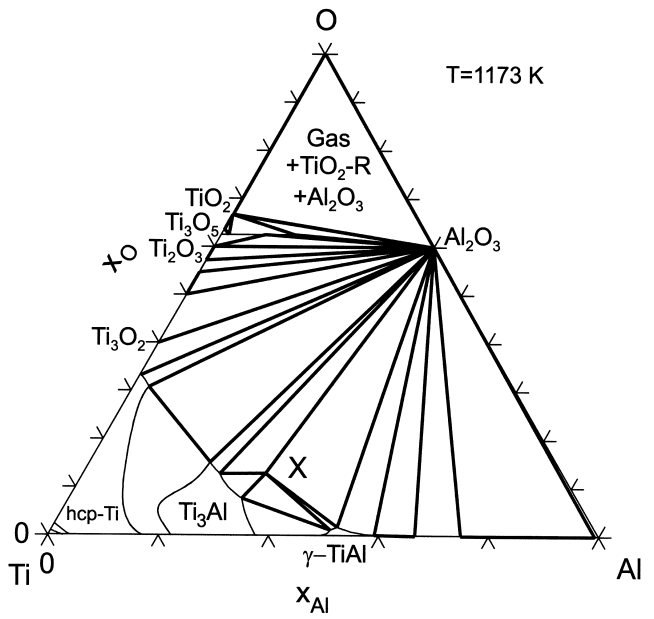

Fig. 3. Isothermal section in the Ti–Al–O system ($T=1173$ K).

3.1. Thermodynamic description of Al_2TiO_5 (aluminum titanate)

To derive the phase diagram shown in Fig. 4, aluminium titanate was modeled on the basis of a sublattice description with occupation of distinct crystallographic positions by Al^{+3}, Ti^{+4} and O^{-2}. The crystallographic positions define the sublattices in the Compound Energy Formalism [17] and assuming Al^{+3} to be located on one distinct position and Ti^{+4} on the other results in the notation: $(Al^{+3})_2(Ti^{+4})_1(O^{-2})_5$.

However, aluminium titanate crystallizes in the so-called pseudobrookite structure (Space Group *Cmcm*) where the cations Al^{+3} and Ti^{+4}, respectively, occupy both positions

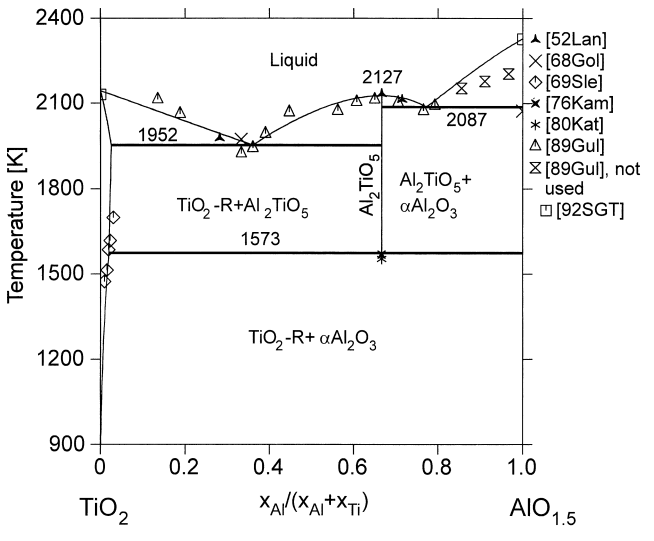

Fig. 4. Optimized phase diagram of the TiO_2–Al_2O_3 system ($p^0=P_{O_2}=1$ bar).

M1 (8*f*) and M2 (4*c*) (i.e. 1st sublattice and 2nd sublattice). Both positions are octahedrally coordinated by oxygen anions (positions 8*f* and 4*c*). The compound energy formalism as described for oxides [18] was used to describe the sublattice model for this case: $(Al^{+3},Ti^{+4})_2(Al^{+3},Ti^{+4})_1(O^{-2})_5$. The corresponding reference part of the Gibbs energy is:

$$
\begin{aligned}
{}^{\mathrm{ref}}G^{Al_2TiO_5} = {} & y'_{Al^{+3}}y''_{Ti^{+4}}\,{}^{0}G_{Al^{+3}:Ti^{+4}} \\
& + y'_{Ti^{+4}}y''_{Al^{+3}}\,{}^{0}G_{Ti^{+4}:Al^{+3}} \\
& + y'_{Al^{+3}}y''_{Al^{+3}}\,{}^{0}G_{Al^{+3}:Al^{+3}} \\
& + y'_{Ti^{+4}}y''_{Ti^{+4}}\,{}^{0}G_{Ti^{+4}:Ti^{+4}}
\end{aligned}
$$

where y'_i and y''_j are the site fractions of the cations for each sublattice separately. This description is based on four end members ('compounds') where three of them are electrically charged and not accessible to experimental investigations: $Al_2Ti_1O_5$ (0), $Ti_2Al_1O_5$ (+I), $Al_2Al_1O_5$ (−I) and $Ti_2Ti_1O_5$ (+II), abbreviated as [A:T4], [T4:A], [A:A] and [T4:T4], respectively (A indicates Al^{+3}, T4 indicates Ti^{+4}). Reciprocal reactions of the end members can be assumed.

The ideal Gibbs energy contribution to the total Gibbs energy of this phase is given by:

$$
\begin{aligned}
{}^{\mathrm{id}}G^{Al_2TiO_5} = {} & -T\,{}^{\mathrm{id}}S \\
= {} & RT[2(y'_{Al^{+3}}\ln y'_{Al^{+3}} + y'_{Ti^{+4}}\ln y'_{Ti^{+4}}) \\
& + (y''_{Al^{+3}}\ln y''_{Al^{+3}} + y''_{Ti^{+4}}\ln y''_{Ti^{+4}})]
\end{aligned}
$$

Single crystal structure investigations of β-Al_2TiO_5 showed that the M1- and M2-positions are randomly occupied by Al^{+3}- and Ti^{+4}-cations [19,20]. Thus the sublattice description can be notated as $(Al^{+3}_{2/3}Ti^{+4}_{1/3})_2(Al^{+3}_{2/3}Ti^{+4}_{1/3})_1(O^{-2})_5$. This random distribution of cations is the configuration of greatest entropy which gives for the ideal Gibbs energy ${}^{\mathrm{id}}G^{Al_2TiO_5} = -15.876\cdot T$ J/(mol K). This energy contribution to the phase stability explains that despite of a positive value of the enthalpy of formation of +25.1 kJ/mol of Al_2TiO_5 at a temperature of 1613 K (calculated value: +23.1 kJ/mol Al_2TiO_5), Al_2TiO_5 is found to be stable at this temperature. Generally, pseudobrookite phases are assumed to be entropy stabilized [21].

The Gibbs energy for one mole of formula units of the phase is described in the Compound Energy Formalism by: $G_m^{\Phi} = {}^{\mathrm{ref}}G^{\Phi} + {}^{\mathrm{id}}G^{\Phi} + {}^{\mathrm{ex}}G^{\Phi}$. No excess Gibbs energy term ${}^{\mathrm{ex}}G^{\Phi}$ had to be taken into account for the description of Al_2TiO_5.

Fig. 5 shows the composition square for the reciprocal model applied to β-Al_2TiO_5 with the four end members defined above. The end members occupy the corners of the square, the axes represent the site fractions of Al^{+3} on the first ($y'_{Al^{+3}}$) and the second ($y''_{Al^{+3}}$) sublattice, respectively. The contour lines link compositions with identical values of ideal Gibbs energies. Only electrically neutral combina-

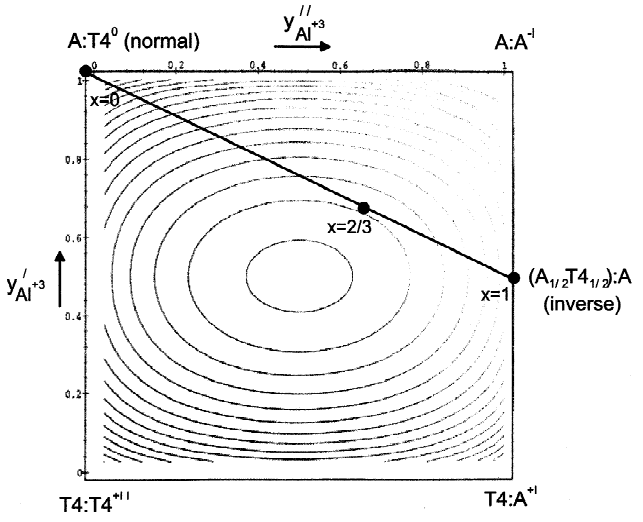

Fig. 5. Composition square for modelling β-Al_2TiO_5 showing the line of electrically neutral compositions. A indicates Al^{+3}, T4 indicates Ti^{+4}.

tions of the compounds have a physical meaning and are located on the indicated line (Fig. 5). The end members of this series, A:T4 (i.e. Al_2TiO_5 (0)) and $A_{1/2}T4_{1/2}$:A (0) are called normal (*N*) and inverse (*INV*) pseudobrookite structures, respectively. Additionally, the mentioned compound with statistical occupation of the crystallographic sites ($x=2/3$) is indicated. Along the neutral line this compound is the most stable one. The four thermodynamic parameters for the indicated square end members can be expressed by only two independent parameters related to the normal and inverse structures, respectively, G_N^{AT} and G_{INV}^{AT}:

$$G_{A:T4} = G_N^{AT}; \quad G_{A:A} = G_{INV}^{AT} + 0.5G_N^{AT};$$
$$G_{T4:A} = G_{INV}^{AT} - 0.5G_N^{AT}; \quad G_{T4:T4} = 0$$

The calculated phase diagram using the model description $(Al^{+3},Ti^{+4})_2(Al^{+3},Ti^{+4})_1(O^{-2})_5$ looks similar as the diagram shown in Fig. 4 (where the description $(Al^{+3})_2(Ti^{+4})_1(O^{-2})_5$ was used) but now the crystal chemistry of β-Al_2TiO_5 is considered.

3.2. Thermodynamic description of the solid solution series Al_2TiO_5–Ti_3O_5

Ti_3O_5 shows, as Al_2TiO_5, a pseudobrookite structure. Both compositions are end members of a complete solid solution series. The end member Ti_3O_5 can be described by a formal exchange of Al^{+3}- by Ti^{+3}-cations which yields a sublattice description $(Ti^{+3},Ti^{+4})_2(Ti^{+3},Ti^{+4})_1(O^{-2})_5$. Similarly, as described for Al_2TiO_5, four end members, a neutral line and a normal and an inverse pseudobrookite structure can be defined. Additionally, similar parameter correlations result:

$$G_{T3:T4} = G_N^{TT}; \quad G_{T3:T3} = G_{INV}^{TT} + 0.5G_N^{TT};$$
$$G_{T4:T3} = G_{INV}^{TT} - 0.5G_N^{TT}; \quad G_{T4:T4} = 0$$

where T3 indicates Ti^{+3}.

The common parameter of Al_2TiO_5 and Ti_3O_5, $G_{T4:T4}$, is arbitrarily set to zero. To describe the solid solution Al_2TiO_5–Ti_3O_5 the sublattice models for Al_2TiO_5 and Ti_3O_5 were combined to $(Al^{+3},Ti^{+3},Ti^{+4})_2(Al^{+3},Ti^{+3},Ti^{+4})_1(O^{-2})_5$. Using reciprocal reactions and constraints on the chemical compositions and electrical neutrality all parameters of the tialite model can be described by the parameters of β-Al_2TiO_5 and α-Ti_3O_5 and two additional parameters:

$$G_{A:T3} = G_N^{AT} + G_{INV}^{TT} - 0.5G_N^{TT};$$
$$G_{T3:A} = G_N^{TT} + G_{INV}^{AT}\, 0.5G_N^{AT}$$

Obviously the total number of nine parameters can be reduced by these relations to four independent ones which had to be adjusted. For details of optimization we refer to [16].

The variation of the cation site fractions in the tialite phase is shown in Fig. 6 ($T=1800$ K). The statistical occupation for Al_2TiO_5 as described above is reproduced as well as the 95%-occupation of position M2 (4*c*) by Ti^{+3} cations in Ti_3O_5 (slightly disordered pseudobrookite structure) as reported by Navrotsky [21]. The bold line indicates the sum of $^{4c}Ti^{+3}$and $^{4c}Al^{+3}$, i.e. $(y''_{Al^{+3}} + y''_{Ti^{+3}})$, which indicates the degree of ordering.

Using the optimized parameters for tialite and the other phases of the Ti–Al–O system isopotential phase diagrams

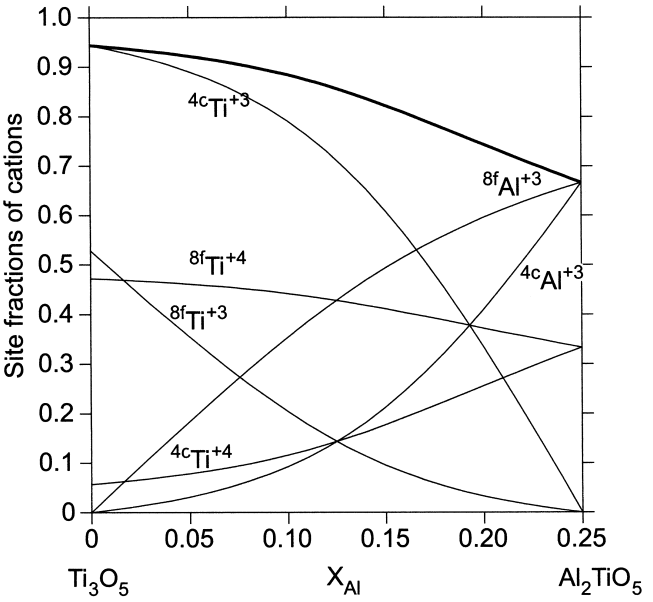

Fig. 6. Site fractions of the cations in the tialite solid solution series Al_2TiO_5–Ti_3O_5 ($T=1800$ K). The bold line indicates the sum of $^{4c}Ti^{+3}$ and $^{4c}Al^{+3}$, i.e. $(y''_{Al^{+3}} + y''_{Ti^{+3}})$, which indicates the degree of ordering.

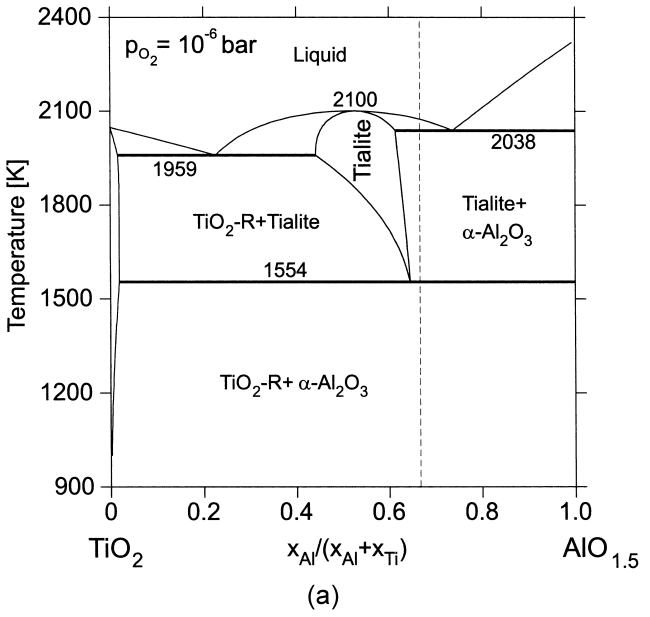

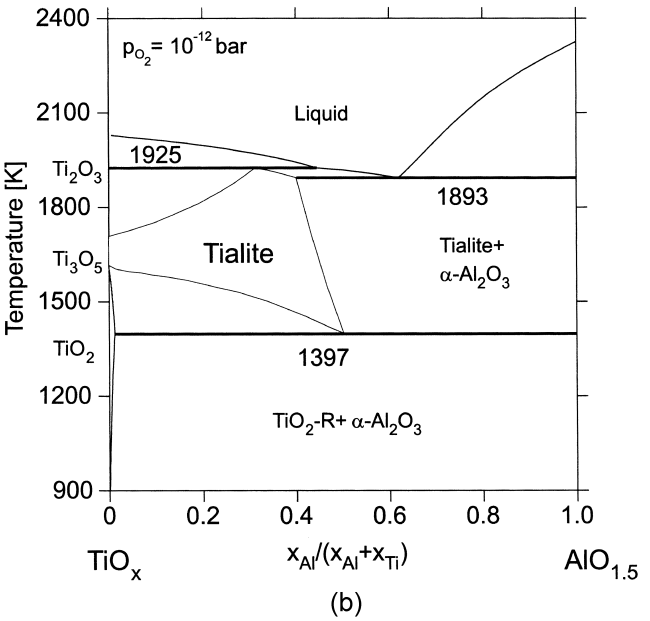

Fig. 7. Optimized isopotential phase diagrams for TiO_x–Al_2O_3. (a) $p^0=1$ bar, $p_{O_2}=10^{-6}$ bar; (b) $p^0=1$ bar, $p_{O_2}=10^{-12}$ bar.

in the system TiO_x–Al_2O_3 were calculated for two different oxygen partial pressures (Fig. 7). Both diagrams illustrate the expanding solid solubility range of the tialite phase when lowering the partial pressure of oxygen. At an oxygen-pressure of $p_{O_2}=10^{-12}$ bar there is a complete solid solubility between Al_2TiO_5–Ti_3O_5 (Fig. 7b).

4. Quaternary system Ti–Al–O–N

The thermodynamic dataset worked out for binary and ternary subsystems of the Ti–Al–O–N system was used to calculate the phase equilibria of arbitrary sections at quaternary compositions. The isopleth AlN–TiO_2 is shown in Fig. 8. The comparison with microstructure analyses of multiphase ceramics derived from sintered powder mixtures of AlN and TiO_2 [1] shows very good agreement. Similar extrapolating calculations can be used as a guideline for the choice of proper powder mixtures and sintering conditions for any ceramics in the Ti–Al–O–N system.

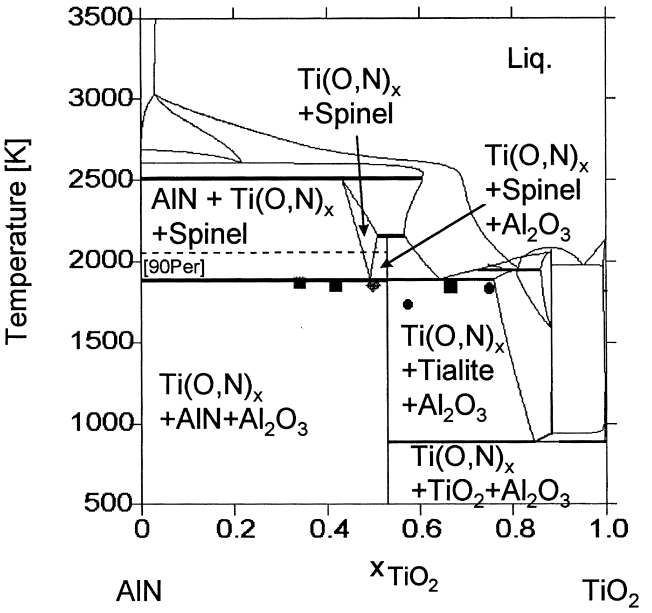

Fig. 8. Calculated AlN–TiO_2 section in the quaternary Ti–Al–O–N system. Experimental data by different authors are indicated.

5. Oxidation of γ-TiAl

The quaternary Ti–Al–O–N dataset was also used to derive information on the oxidation behavior of γ-TiAl and related diffusion paths.

The term ‘diffusion path’ is defined as average composition along the diffusion zone in planes normal to the diffusion direction [22]. In a phase diagram it is indicated by a line connecting all (measured) compositions i.e. chemical potentials between phases combined initially. The path reflects the thermodynamic equilibria at the phase boundaries in the diffusion zone and is time independent. However, during the diffusion process the layer sequence may alter as phases form or disappear. Therefore, paths for intermediate states are shown in this work as well.

During the oxidation of metallic γ-TiAl in air alumina and other phases (e.g. TiN, Ti_2AlN) are formed at the surface. The alumina formation leads to an Al-depleted sub-surface zone within γ-TiAl. This sub-surface layer plays an important role for the mechanical and oxidation properties of γ-TiAl. The light-optical micrographs and microprobe investigations show the surface layer after 100 h of oxidation at 1173 K in air (Fig. 9). The formation of

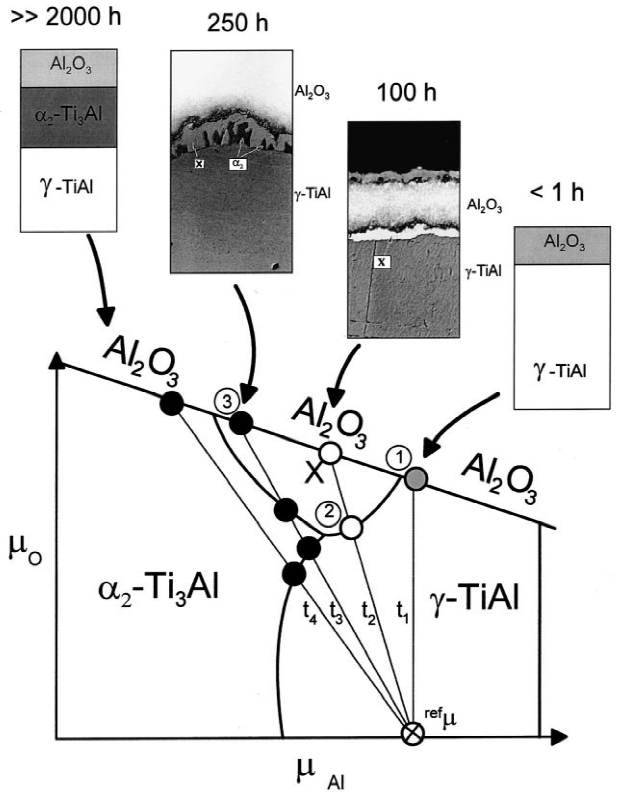

Fig. 9. Light-optical images of the γ-TiAl oxidation zone and Ti–Al–O potential phase diagram (1173 K and $p^0 = 1$ bar) with indicated (diffusion) paths.

the above-mentioned ternary X-phase (Fig. 3) can be seen. After 250 h of oxidation additionally α_2-Ti_3Al has formed. Extended oxidation times show the disappearance of the X-phase.

To understand this oxidation behavior the potential phase diagram at a temperature of 1173 K was calculated neglecting the nitrogen effect in a first step (Fig. 9). The corresponding isothermal section is shown in Fig. 3. The chemical potentials of oxygen and aluminum, respectively, were used as axes, since, as known by experiments, oxygen and aluminum are the main diffusing components during the formation of the sub-scale zone [2]. The potential phase diagram shows areas of single phases and lines and points of two phase and three phase equilibria, respectively. It can be used for a first analysis of the phase evolution of the diffusion-controlled process of γ-TiAl oxidation for two reasons: (1) chemical potential gradients are the driving forces for diffusion and (2) local equilibria at the interfaces of the phases can be assumed. For sake of simplicity a linear variation of the chemical potentials along the diffusion zone was assumed. The change of the chemical potentials of aluminum and oxygen through the diffusion zone can then be described by an iterative formula $\mu_{i+1}(\mathrm{Al})(t) = \mu_i(\mathrm{Al}) + \Delta\mu(\mathrm{Al})(t)$ and $\mu_{i+1}(\mathrm{O}) = \mu_i(\mathrm{O}) + \Delta\mu(\mathrm{O})$, respectively, with $\Delta\mu(\mathrm{O}) > 0$ and $\Delta\mu(\mathrm{Al}) < 0$ where the index i is equivalent to a distance within the alloy. Oxygen is a fast diffusing component [2]. Therefore, the time dependence of the step value $\Delta\mu(\mathrm{O})$ was neglected. The step value for aluminum can then be related with $\Delta\mu(\mathrm{O})$ by a time-dependent model parameter $q(t)$: $\Delta\mu(\mathrm{O})/\Delta\mu(\mathrm{Al})(t) = q(t)$ with $-\infty < q(t) < 0$.

The parameter $q(t)$ defines the paths indicated in the potential phase diagram in Fig. 9 at a time t. It defines the slope of a straight line which starts at ${}^{\mathrm{ref}}\mu$ assuming very small oxygen impurities in γ-TiAl. With these assumptions the oxidation process of γ-TiAl can be described as a series of successive local equilibria states t_1 to t_4. Path t_1 defines the start of the oxidation with γ-TiAl(O) and Al_2O_3 in equilibrium. Path t_2 predicts the evolution of the interfaces Al_2O_3/X and γ-TiAl(O)/X in good accordance with the kind of surface layers found after 100 h of oxidation. The oxidation experiments show that after 250 h additionally α_2-Ti_3Al has formed which is simulated by path t_3. Path t_4 (the 'diffusion path' according to definition in [22]) predicts the final state of oxidation at which the X-phase disappeared completely after extended time periods of oxidation. Thus from the disappearance of the X-phase during oxidation of γ-TiAl it cannot be concluded that it is a metastable phase. These calculations are described in detail in [23].

To take into account the nitrogen diffusion during oxidation in air, a potential phase diagram in the Ti–Al–O–N system for a temperature of 1173 K was calculated (Fig. 10). The chemical potentials of oxygen and nitrogen were used as axes at a fixed ratio $x_{\mathrm{Al}}/x_{\mathrm{Ti}} = 1$. The layer of Al_2O_3 and titaniumnitrides experimentally found can be explained by using this diagram [16]. Starting from the interface oxide/gas in the upper right corner of the diagram, the partial pressures of oxygen and nitrogen

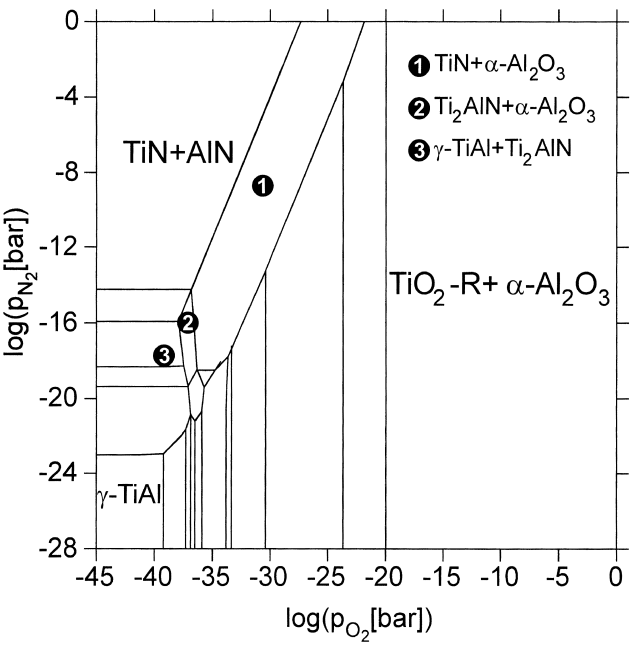

Fig. 10. Ti–Al–O–N potential phase diagram at $x_{\mathrm{Al}}/x_{\mathrm{Ti}} = 1$.

decrease continuously to the direction of the interface between metal and the oxide. Phase field 1 shows the stability field for TiN and Al_2O_3, field 2 the equilibrium Ti_2AlN–Al_2O_3, and field 3 the equilibrium γ-TiAl–Ti_2AlN, confirming the experimental results on the phase assemblages in surface layers of γ-TiAl oxidized in air [2].

6. Conclusions

It was demonstrated that an internally consistent dataset is useful to simulate phase equilibria and phase reactions of multiphase materials in the Ti–Al–O–N system. Modeling of solution phases on the basis of crystal structure and crystal chemistry is crucial for the calculation of ceramic and metallic systems using phase diagram data and thermodynamic data. The sublattice model described in the Compound Energy Formalism can be successfully used to treat solid and liquid solution phases as has been demonstrated with the tialite solid solution Al_2TiO_5–Ti_3O_5. Various types of computed phase diagrams as: (1) binary temperature–composition diagrams, (2) ternary isothermal sections, (3) ternary (isopotential) temperature–composition diagrams and (4) potential phase diagrams are useful to explain the microstructure and oxidation behavior of such materials.

A simple thermodynamic model can be used to simulate diffusion processes and explain the thermal oxidation process of γ-TiAl. The potential phase diagrams with indicated diffusion paths allow a comparison of local thermodynamic equilibria and experimental results. The model enable calculations predicting thermodynamically possible layer sequences.

Acknowledgements

For helpful discussions we thank H.L. Lukas and J. Golczewski. M. Thomas is thanked for support in preparing this manuscript.

References

[1] D.S. Perera, Br. Ceram. Trans. 89 (1990) 57.
[2] F. Dettenwanger, E. Schumann, M. Rühle, J. Rakowski, G.H. Meier, Oxidation of Metals 50 (1998) 269.
[3] N. Saunders, P. Miodownik, in: R.W. Cahn (Ed.), CALPHAD (Calculation of Phase Diagrams): A Comprehensive Guide, Materials Series, Vol. 1, Pergamon, Oxford, 1998.
[4] H.J. Seifert, F. Aldinger, Z. Metallkd. 87 (1996) 841.
[5] H.L. Lukas, S.G. Fries, J. Phase Equilibria 13 (1992) 532.
[6] B. Sundman, B. Jansson, J.-O. Andersson, CALPHAD 9 (1985) 153.
[7] N. Saunders, System 'Al–Ti', COST507, in: I. Ansara, A.T. Dinsdale, M.H. Rand (Eds.), Thermochemical Database For Light Metal Alloys, European Commision, Luxembourg, 1998.
[8] K. Zeng, R. Schmid-Fetzer, Z. Metallkd. 87 (1996) 540.
[9] B. Hallstedt, J. Am. Ceram. Soc. 75 (1992) 1497.
[10] Scientific Group Thermodata Europe, Grenoble Campus, 1001 Avenue Centrale, BP66, F-38402 Saint Martin D'Heres, France, http://www.sgte.org
[11] B.-J. Lee, J. Korean Inst. Met. Mater. 32 (1994) 869.
[12] H.L. Lukas, 'System Al–N', COST507, in: I. Ansara, A.T. Dinsdale, M.H. Rand (Eds.), Thermochemical Database For Light Metal Alloys, European Commision, Luxembourg, 1998.
[13] B.-J. Lee, N. Saunders, Z. Metallkd. 88 (1997) 152.
[14] K. Zeng, R. Schmid-Fetzer, Thermodynamic modeling and applications of the Ti–Al–N phase diagram, in: Y.A. Chang, F. Sommer (Eds.), Proceedings of the Hume–Rothery Symposium on Thermodynamics of Alloy Formation, Orlando, Florida, Feb. 9–12, 1997, The Minerals, Metals and Materials Society, Warrendale, PA, 1997, p. 275.
[15] L. Dumitrescu, B. Sundman, J. Europ. Ceram. Soc. 15 (1995) 239.
[16] A. Kussmaul, Thermodynamische Berechnungen zum Einfluss reduzierender und oxidierender Atmosphären auf Werkstoffe im System Ti–Al–O–N, Dissertation, Universität Stuttgart, 1998.
[17] J.-O. Andersson, A. Fernandez Guillermet, M. Hillert, B. Jansson, B. Sundman, Acta Metall. 34 (1986) 437.
[18] T.I. Barry, A.T. Dinsdale, J.A. Gisby, B. Hallstedt, M. Hillert, B. Jansson, S. Jonsson, B. Sundman, J.R. Taylor, J. Phase Equilibria 13 (1992) 459.
[19] B. Morosin, R.W. Lynch, Acta Crystallogr. B28 (1972) 1040.
[20] T. Epicier, G. Thomas, H. Wohlfromm, J.S. Moya, J. Mater. Res. 6 (1991) 138.
[21] A. Navrotsky, American Mineralogist 60 (1975) 249.
[22] F.J.J. van Loo, Prog. Solid St. Chem. 20 (1990) 47.
[23] A. Kussmaul, H.J. Seifert, J.A. Golczewski, H.L. Lukas, F. Aldinger, Z. Metallkd. 89 (1998) 683.